IEEE Access
Multidisciplinary | Rapid Review | Open Access Journal

Date of publication xxxx 00, 0000, date of current version xxxx 00, 0000.

*Digital Object Identifier 10.1109/ACCESS.2017.DOI*

# Circuit model of Parallel Corrugated Transmission Lines for Differential Signal Propagating in Microwave Band

**CHIA HO WU[1], GUOBING ZHOU[1],JEHN-YIH JUNG[2],QIAN SHEN[1],YUN YOU[1],JINHUA YAN[1],LINFANG SHEN[1],HANG ZHANG[1],YU WU[1],FANGMING ZHU[3], AND CHIN CHIH CHANG.[4]**

[1]Department of Applied Physics, College of Science, Zhejiang University of Technology, Hangzhou 310023, China
[2]Department of Electrophysics, National Chiao Tung University, Hsinchu 30012, Taiwan
[3]College of Information Science and Engineering, Hangzhou Normal University, Hangzhou 311121, China
[4]Department of Computer Science and Information Engineering, Chung Hua University, Hsinchu 30012, Taiwan

Corresponding authors: L. Shen (e-mail: lfshen@zjut.edu.cn) and H. Zhang (e-mail: physzhang@zjut.edu.cn).

This work was support by the National Natural Science Foundation of China under Grant 62075197 and the Science Foundation of Zhejiang Province under Grant LY17F010010,LQ21F010013.

**ABSTRACT** A viable wide-band circuit model of parallel corrugated differential transmission line is established. By solving for the even- and odd-modes in this structured differential transmission line, the equivalent capacitance, inductance, resistance, and conductance per unit length are calculated, then the characteristic impedances of differential and common signals are obtained. The *S*-parameters obtained from the equivalent circuit model agree well with the full-wave simulation results with a deviation of only about 0.036 dB in the frequency range of 10 GHz. Experimentally, the characteristic impedances are measured for the differential and common signals using a time domain reflectometer (TDR). The deviation between the experimental and theoretical results was less than 1.05%. Based on the equivalent circuit model, it is feasible to implement this type of structured differential line directly into real circuits.

**INDEX TERMS** Corrugated transmission lines, crosstalk, differential signal.

## I. INTRODUCTION

WITH higher frequency and smaller circuit board area, the crosstalk between adjacent transmission lines becomes much more serious. Such problem has been studied widely using the finite-difference time-domain (FDTD) and equivalent circuit model method [1]– [3]. A simple way to suppress the crosstalk is keeping the separation distance between transmission lines considerably larger than the line width [4], and the variation of *S*-parameters for different separation distances was discussed in [5]. However, as the signal frequency increases, this method fails, because it becomes more difficult to reduce circuit board area. New methods to suppress crosstalk at far and near ends are put forward. In [6], the dielectric substrate between transmission lines is removed to decrease crosstalk. Introducing a nonuniform transmission line between two microstrip lines is another way to restrain signal coupling [7], but it restricts the miniaturization of the circuit board. In order to reduce electromagnetic interference between two microstrip lines, in [8] a way of connecting two parallel transmission lines with a decoupling capacitor to control the even- and odd-mode capacitances was proposed. The most commonly used means to cancelling the far end crosstalk is adding grounded guard trace between signal microstrip lines [9]– [15]. However, it was pointed out that there may exist resonating effect when the grounded rods are distributed inappropriately [14]. These grounded guard traces are also used in differential transmission lines [16]. However, the grounded guard traces still have the problem of greater area.

Periodic structures are introduced in microstrip lines to adjust the ratio of mutual capacitance and inductance to control electromagnetic interference [17], which has the advantage of smaller interval. For the scheme of suppressing far-end crosstalk between two microstrip lines with interdigital trapezoid tabs, quasi-static analysis was made and compared with the results of the full-wave calculation [18]. In [19], some extended formulas were used to determine the relationship of distribution parameters of symmetry and asymmetry interconnects with frequency and temperature. Based on the quasi-static analysis, a circuit model was built for coplanar

This article has been accepted for publication in a future issue of this journal, but has not been fully edited. Content may change prior to final publication. Citation information: DOI 10.1109/ACCESS.2020.3044322, IEEE Access



symmetrical meander lines and the relevant parameters were extracted [20]. Step shaped microstrip lines with reduced crosstalk have been studied in [21]. The effect of suppressing crosstalk in subwavelength periodic corrugated microstrip lines has been verified in [22], [23]. Discontinuous structured guard lines can be used to adjust the mutual capacitance and inductance between periodically loaded transmission lines to suppress far-end crosstalk [24]. The differential microstrip lines consist of two parallel and equal length microstrip lines with the $180^\circ$ phase difference between them. Comparing with the single-ended driver, the *dI*/*dt* of the differential output driver is significantly suppressed, hence the potential electromagnetic interference (EMI) can be substaintially reduced. In some real circuits, it has been demonstrated that the strongly-coupled differential microstrip lines exhibit a much smaller crosstalk interference with the neighboring circuits than that of the single-ended microstrip lines. In addition, the differential amplifier has a much higher gain than the single-ended amplifier [4]. Consequently, recently more and more planar single-ended microstrip lines have been replaced by the differential ones. However, with the ever increasing demands in CPU signal transmission speed, the coupling effect between conventional differential microstrip line (CDML) and neighboring circuit is rapidly increased and lead to unsatisfactory noise level. Moreover, the asymmetric circuit distribution existing on both sides of the CDML may also lead to serious common signal effect. For differential pair, the differential signal excites the odd-mode of the coupled transmission lines, and the common signal excites the even-mode. Due to manufacturing errors, the introduction of undesired asymmetries and nonuniformities will cause unnecessary common signal effects in the differential transmission lines, and this issue has been discussed in detail in [25]. Under the condition of weak coupling, the mechanism of common-mode noise generation was studied when the transient signal is transmitted along differential serpentine delay lines, and an accurate circuit model was proposed [26].

Recently, by introducing subwavelength periodic structure, a new kind of differential microstrip lines has been demonstrated to exhibit substantial suppression on coupling and common signal effect, compared to CDML [27], [28]. Usually, a planar circuit contains many active devices and transmission lines (or interconnections). The transmission characteristics of these interconnections can be accurately solved by full-wave simulation with commercial software. When the equivalent circuit parameters are extracted from the simulated results for these interconnections, they can be easily combined with the equivalent circuit of active devices for SPICE analysis. In [27], it was clearly pointed out that the subwavelength periodic differential microstrip lines show extremely strong reduction of the far-end crosstalk and suppress the undesired common signal effect. If such transmission lines are applied in actual circuits and combined with active devices, it is necessary to provide sufficiently accurate circuit parameters of subwavelength periodic differential microstrip lines. In addition, in order to be used in the actual planar circuit, it is also necessary to further calculate the differential signal and common signal impedances from the obtained circuit parameters. By properly choosing the lattice constant and groove depth of the subwavelength periodic structure, one can design the coupling strength between the two structured microstrip lines. And by the method proposed in this paper, the mutual capacitance and mutual inductance of the coupled microstrip lines can be calculated, and these have physical characteristics completely different from that of the single subwavelength periodic microstrip line. Because the property of coupling between subwavelength periodic microstrip lines is completely different from that between two conventional microstrip lines, it is necessary to carefully study the characteristics of the differential circuit formed by subwavelength periodic microstrip lines.To our knowledge, the circuit parameters of differential subwavelength periodic microstrip lines are proposed for the first time. Moreover, it is very important to further establish a complete circuit model for the practical applications.

In this paper, by following the basic definitions, the equivalent circuit parameters of the unilaterally structured differential microstrip lines were simulated using the finite element method. The results indicate that the equivalent capacitance ($C$), resistance ($R$), conductance ($G$), and inductance ($L$) are closely dependent on frequency. With the obtained equivalent circuit parameters ($C(f)$, $L(f)$, $R(f)$ and $G(f)$), the characteristic impedances of differential and common signals are then obtained. To validate the circuit model, the *S*-parameters of the differential and common signals of a DML composed of two 10 cm-long subwavelength periodic microstrip lines were calculated, and were further compared with those obtained from the full-wave simulations. The excellent agreement between the *S*-parameters are found, so the equivalent circuit parameters provide valuable information for directly implementing structured differential microstrip lines in printed circuit board (PCB) design.

## II. THEORETICAL ANALYSIS

The unilateral subwavelength periodic differential microstrip line (USPDML) consisting of two coupling corrugated microstrip lines under consideration is shown schematically in Fig. 1(a). The two microstrip lines have the same geometric parameters: the line width *w*, subwavelength lattice constant *d*, substrate thickness *h*, metal thickness *t*, groove depth *b*, groove width *a* and the substrate has the dielectric constant $\varepsilon_r$. The USPDML is fed with two signals with $180^\circ$ phase difference.

The USPDML is a one-dimensional periodic structure, and the unit cell is a section of it whose length is equal to the period. The period is also called lattice constant, and it is on subwavelength scale for the USPDML. The equivalent circuit of the coupled subwavelength periodic microstrip lines is shown in Fig. 1(b). Here, the resistance of the metal and the conductance of the substrate dielectric are omitted. Through the analysis with the commercial software COMSOL, it is easy to obtain the distributions of electric and magnetic field

This article has been accepted for publication in a future issue of this journal, but has not been fully edited. Content may change prior to final publication. Citation information: DOI 10.1109/ACCESS.2020.3044322, IEEE Access



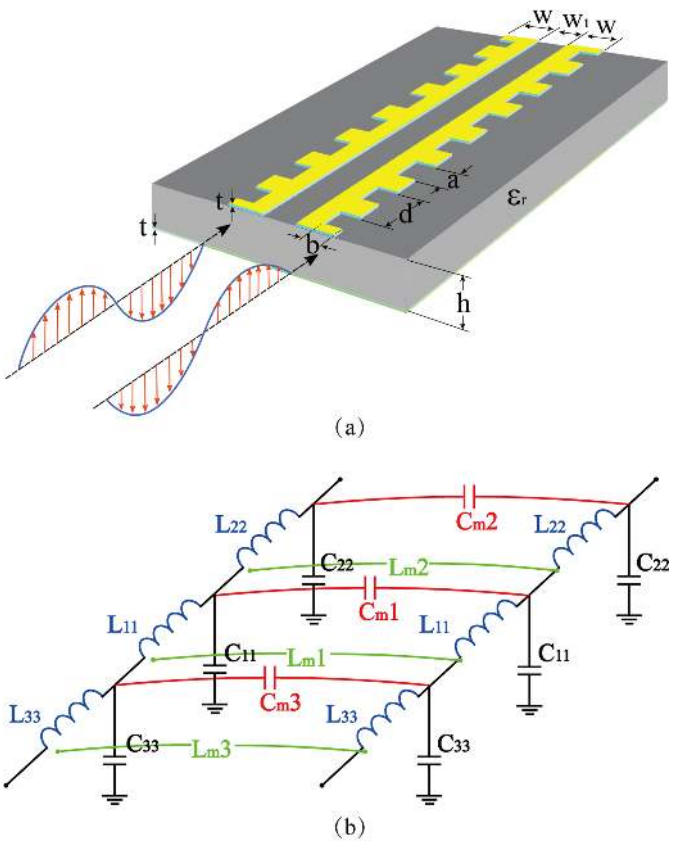


**FIGURE 1.** (a) Schematics of the unilateral subwavelength periodic differential microstrip line (USPDML). (b) The equivalent circuit of coupled microstrip lines for a unit cell.

lines in the coupled subwavelength periodic microstrip lines at different frequencies. In the frequency range of 0–15 GHz, almost all magnetic field lines are closed around the direction of the transmission line, and there are no closed magnetic field lines in the plane vertical to the metal rectangle tabs. It can be evaluated that under the quasi-static condition, there is no need to introduce extra inductance along the tab. There are almost no interconnected electric field lines in the two rectangle tabs of groove, so there is no need to introduce extra capacitance as well. Therefore, the equivalent circuit of the subwavelength periodic structure is the same as that of the conventional coupled microstrip lines. The capacitance and inductance of the USPDML were extracted from the solutions of respective modes. In the present example, RO4003 ($\varepsilon_r = 3.37$) with thickness $h = 0.508$ mm is chosen as the substrate. The metal stripes have thickness $t = 0.0175$ mm, line width $w = 1.2$ mm, groove depth $b = 0.6\ w$, lattice constant $d$, interval between strip $w_1$ and groove width $a = 0.5\ d$, respectively.To make two microstrip lines to be strongly coupled with each other, the interval between them is set at $w_1 = w$. Figs. 2 (a) and (b) show the dispersion curves of odd- and even-modes for the lattice constant $d = 0.5$ mm, respectively. The asymptotic frequency evaluated at the Brillouin edge (i.e., $\beta = \pi/d$) gives $f_{so} \approx f_{se} = 59.329$ GHz for the odd- and even-mode, respectively. The

**TABLE 1.** The odd- and even-mode asymptotic frequencies for USDMLs with different lattice constants.

| d (mm) | Mode | $f_{so}$ (GHz) | Mode | $f_{se}$ (GHz) |
|---|---|---|---|---|
| 0.5 | Odd | 59.329 | Even | 59.329 |
| 1.0 | Odd | 48.958 | Even | 48.946 |
| 2.0 | Odd | 33.184 | Even | 32.772 |

two dispersion curves almost overlap each other. Similarly, Figs. 2 (c) and (d) show results for $d = 1.0$ mm, which give the asymptotic frequency of $f_{so} = 48.958$ GHz and $f_{se} = 48.946$ GHz for the odd- and even-mode, respectively. For the case $d = 2.0$ mm, the asymptotic frequencies are found to be $f_{so} = 33.184$ GHz and $f_{se} = 32.772$ GHz for the odd- and even-mode, respectively. The results are summarized and listed in Table 1.

Since the lattice constant $d$ of the USPDML is much smaller than the signal wavelength $\lambda$ in free space. In the low frequency approximation, the equivalent circuit model of uniform transmission line can be directly applied. At this time, the phase velocity $v_p$ and characteristic impedance $Z_o$ of subwavelength periodic structure can be approximated as [29]:

$$v_p \approx \frac{1}{\sqrt{LC}} \tag{1}$$

and

$$Z_o \approx \sqrt{\frac{L}{C}} \tag{2}$$

where $C$ and $L$ are the capacitance and inductance per unit length, respectively. The total electric charge $Q$ accumulated on the surface of the periodic microstrip line can be calculated by taking a closed surface around the periodic microstrip line. The voltage $V_o$ can be obtained by integrating the electric field between the signal trace and the return path. In order to improve the accuracy of the calculation, the unit cell of the periodic structure is divided into many sub-regions, and the respective capacitances are calculated in each sub-region. The value of the capacitance can be obtained by the ratio of the charge accumulated on the surface of the signal trace to the voltage. The value of the inductance can be obtained by the ratio of the magnetic flux linkage with the signal trace and the surface current. All computations are carried out in a unit cell of the periodic structure by using COMSOL. The above formulas are valid at low frequencies as the subwavelength periodic corrugation structure has the effect of low-pass filtering. However, for comparison, the variation of equivalent circuit parameters with frequency is still calculated near the asymptotic frequency. Fig. 3 shows the magnetic field amplitudes of odd-mode at the asymptotic frequency for the USPDML with $d = 1.0$ mm. It is evident that the magnetic field is better confined with larger groove depth, as shown in Fig. 3(c), where the upper panel is the magnetic field distribution in the vertical slice halving the groove, and the lower one is the magnetic field distribution in the horizontal slice at the interface of the groove and substrate in the unit cell.

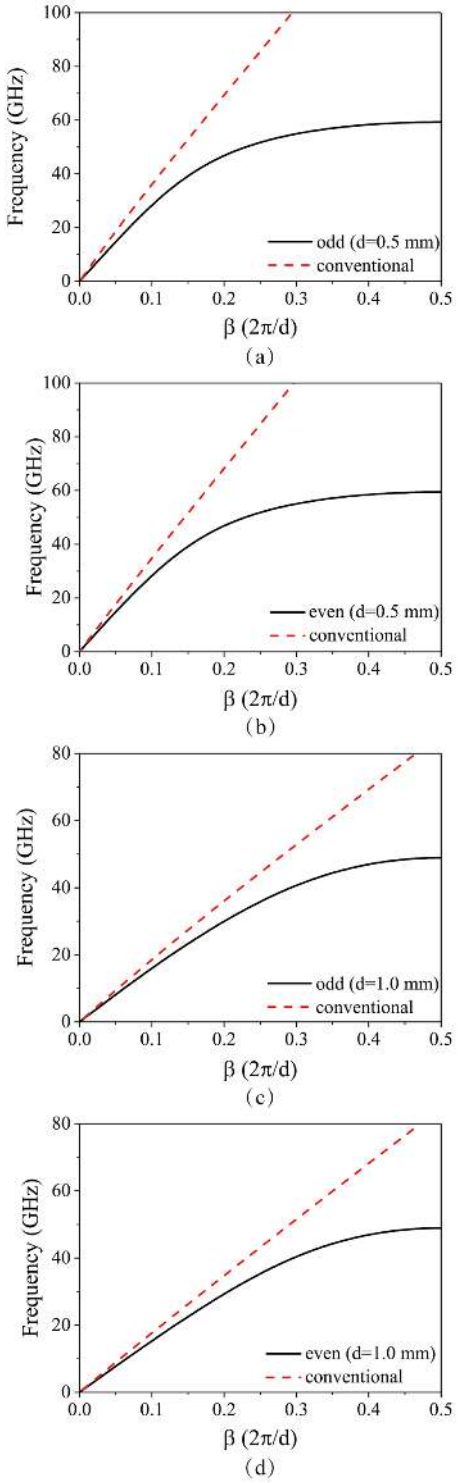


**FIGURE 2.** Dispersion curves for USPDMLs. (a) Odd-mode for d=0.5 mm, (b) even-mode for d=0.5 mm, (c) odd-mode for d=1.0 mm, and (d) even-mode for d=1.0 mm.

The capacitance and inductance per unit length of the USPDML are calculated using the finite element method (FEM) in a unit cell and the results are shown in Fig. 4. For comparison, the numerical results of a conventional differential microstrip line (CDML) are also included as pink dashed curves. As can be seen from Fig. 4(a), for the CDML, the capacitance per unit length for the odd-mode is $C_{odd}$ = 0.11468 pF/mm at $f$ = 0.03773 GHz, and it decreases

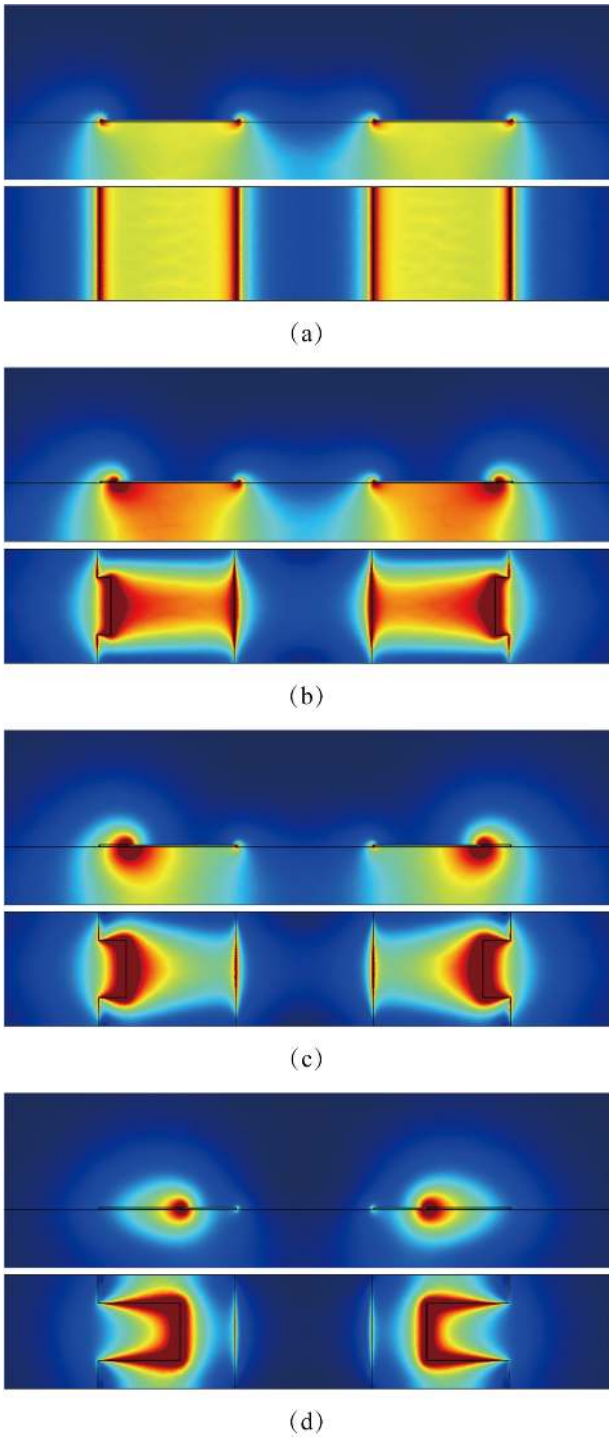


**FIGURE 3.** Magnetic field distributions of odd-mode in the vertical (upper panel) and horizontal (lower panel) slices halving the groove in the unit cell. (a) The conventional differential line, (b)-(d) the USPDMLs with b=0.1w, 0.2w, and 0.6w, respectively.

This article has been accepted for publication in a future issue of this journal, but has not been fully edited. Content may change prior to final publication. Citation information: DOI 10.1109/ACCESS.2020.3044322, IEEE Access



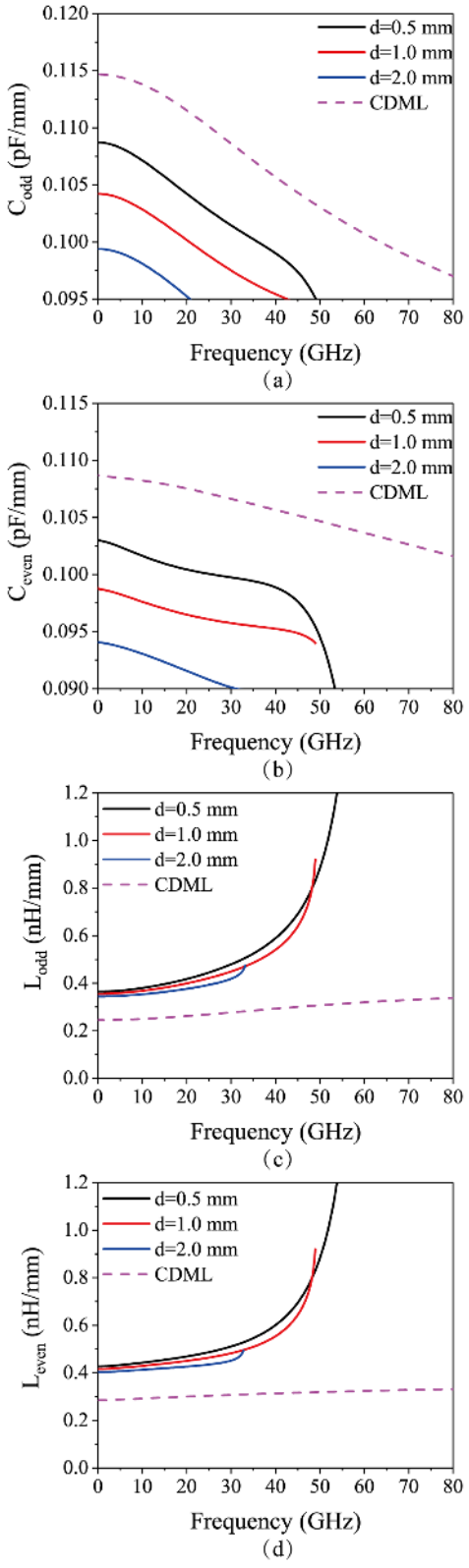


**FIGURE 4.** Per unit length capacitance and inductance of USPDML. (a), (b) Capacitances for odd- and even-modes; (c), (d) inductances for odd- and even-modes.

slowly to $C_{odd} = 0.09402$ pF/mm at $f = 100$ GHz. The variation over the entire frequency range (0−100 GHz) is about 18%. On the other hand, due to the subwavelength periodic corrugation, the $C_{odd}$ is smaller for the USPDML. For the case of $d = 0.5$ mm, the value of the capacitance per unit length has a maximum of $C_{odd} = 0.10874$ pF/mm at $f = 0.03177$ GHz, and drops to $C_{odd} = 0.06802$ pF/mm at the asymptotic frequency $f_{so} = 59.329$ GHz. The variation over the working band is about 37.4%. Similarly, for $d = 1$ mm, the value is $C_{odd} = 0.10423$ pF/mm at $f = 0.01642$ GHz, and drops to $C_{odd} = 0.09364$ pF/mm at the asymptotic frequency $f_{so} = 48.958$ GHz and, for $d = 2$ mm, $C_{odd} = 0.09939$ pF/mm at $f = 0.00854$ GHz, which drops to $C_{odd} = 0.09114$ pF/mm at $f_{so} = 33.184$ GHz. Apparently, the $C_{odd}$ decreases with the increasing lattice constant. For the even-mode (Fig. 4(b)), the $C_{even}$ of the CDML shows a maximum value of $C_{even} = 0.10871$ pF/mm at $f = 0.03593$ GHz, which decreases to $C_{even} = 0.09959$ pF/mm at $f = 100$ GHz with a smaller variation range as compared to that for the odd-mode. For the USPDML with $d = 0.5$ mm, $C_{even} = 0.10301$ pF/mm at $f = 0.03015$ GHz, which decreases to $C_{even} = 0.09849$ pF/mm at $f = 39.592$ GHz, and then drops rapidly to $C_{even} = 0.06803$ pF/mm at the asymptotic frequency $f_{se} = 59.329$ GHz. For the cases of $d = 1.0$ mm and $d = 2.0$ mm, the maximum values of the $C_{even}$ are $C_{even} = 0.09886$ pF/mm at $f = 0.01559$ GHz and $C_{even} = 0.09408$ pF/mm at $f = 0.00812$ GHz, respectively. The results displayed above indicate that the capacitance per unit length not only depends strongly on the frequency, but also very much dependent on the actual geometric structure of the USPDML, which, in turn, suggests the necessity of an efficient means for obtaining the equivalent circuit parameters for real circuit design.

Fig. 4(c) shows the inductance per unit length for odd-mode of the coupled microstrip lines. For the CDML, the inductance per unit length for odd-mode has a minimum of $L_{odd} = 0.24516$ nH/mm at $f = 0.03773$ GHz, then increases slowly to $L_{odd} = 0.35051$ nH/mm at the frequency $f = 100$ GHz, with quite narrow variation range in the whole band. For the USPDML with $d = 0.5$ mm, the $L_{odd}$ has a minimal value $L_{odd} = 0.36464$ nH/mm at $f = 0.03177$ GHz, then increases slowly to $L_{odd} = 0.4843$ nH/mm at $f = 30.628$ GHz. Beyond 30 GHz, it grows sharply to $L_{odd} = 4.2592$nH/mm at $f_{so} = 59.329$ GHz, indicating about eleven folds of increase in self-inductance within the frequency range studied. Apparently, the subwavelength periodic corrugation structure has led to substantial coupling with the magnetic field above the frequency $f = 30$ GHz, leading to much greater inductance over the CDML. For $d = 1.0$ mm, the $L_{odd}$ has a minimal value of $L_{odd} = 0.35529$nH/mm at $f = 0.01642$GHz and increases gradually to $L_{odd} = 0.92025$ nH/mm at the asymptotic frequency $f_{so} = 48.958$ GHz. It also shows about 2.59 times increase over the frequency range studied. In contrast, for d = 2.0 mm, $L_{odd} = 0.3443$ nH/mm at $f = 0.00854$ GHz, then increases to $L_{odd} = 0.47416$ nH/mm at the asymptotic frequency $f_{so} = 33.184$ GHz. In this case, the increase in

This article has been accepted for publication in a future issue of this journal, but has not been fully edited. Content may change prior to final publication. Citation information: DOI 10.1109/ACCESS.2020.3044322, IEEE Access



$L_{odd}$ is only less than 1.38 times over the frequency range approaching the asymptotic frequency. Fig. 4(d) shows the inductance per unit length of even-mode for CDML and USPDML. For the CDML, $L_{even} = 0.28519$ nH/mm at $f = 0.03593$ GHz, then increases slowly to $L_{even} = 0.33626$ nH/mm at $f = 100$ GHz. The variation, similar to the odd-mode, is only about 15%. However, for the USPDML with $d = 0.5$ mm, the $L_{even}$ has a minimum of $L_{even} = 0.42714$ nH/mm at $f = 0.03015$GHz, and increases to $L_{even} = 4.2594$ nH/mm at the asymptotic frequency $f_{se} = 59.329$ GHz. For the cases $d = 1.0$ mm and $d = 2.0$ mm, the minimal values of $L_{even}$ are $L_{even} = 0.41611$ nH/mm at $f = 0.01559$ GHz and $L_{even} = 0.40324$ nH/mm at $f = 0.00812$ GHz, respectively.

A closer inspection for the case of $d = 0.5$ mm in the USPDMLs reveals that, despite that $C_{odd}$ and $C_{even}$ has a maximum difference of approximately 0.00056 pF/mm at frequencies above 40 GHz, both $L_{odd}$ and $L_{even}$ are nearly the same frequency range (over 40 GHz). These observations strongly imply that the two parallel microstrip lines are having very weak coupling between each other as the frequency is increased and the two fed-in signals are essentially transmitting independently. Therefore, for the USPDML, the coupling effect of the two microstrip lines gradually weakens as the frequency increases. On the contrary, the two conventional microstrip lines have a strong coupling effect in the whole frequency range under consideration. In [18], FEXT is effectively eliminated by introducing interdigital trapezoidal tabs between two coupled microstrip lines. In order to verify the feasibility of our method, the example proposed in [18] is analyzed. Because each microstrip line has periodic trapezoidal tabs, the microstrip line is divided into many sub-regions according to the required accuracy. The accumulated charge in each sub-region on the microstrip surface can be obtained through surface integration, and it is further divided by the potential difference between the signal trace and the return path, then the capacitance of each sub-region is evaluated. Similar operations can be used to calculate the inductance. As for the mutual capacitance and mutual inductance, it can be solved by using the capacitance and inductance matrices.

With the obtained capacitance and inductance per unit length, the odd-mode and even-mode characteristic impedances can be calculated using [4]

$$Z_{odd} = \sqrt{\frac{L_{odd}}{C_{odd}}} \tag{3}$$

and

$$Z_{even} = \sqrt{\frac{L_{even}}{C_{even}}} \tag{4}$$

Fig. 5 displays the odd-mode and even-mode characteristic impedances of the USPDML with different lattice constants. The characteristic impedance of the CDML is also plotted with pink and green dashed lines for comparison, which are obtained from the FEM and *LineCalc* simulations, respectively. From Fig. 5(a), it can be seen that the odd-mode characteristic impedance of the CDML increases slowly from minimum numerical value $Z_{odd} = 46.236\ \Omega$ at $f = 0.03773$ GHz to $Z_{odd} = 59.142\ \Omega$ at $f = 80.735$ GHz. For the USPDML with $d = 0.5$ mm, the odd-mode characteristic impedance is $Z_{odd} = 57.908\ \Omega$ at $f = 0.03177$ GHz, which increases to $Z_{odd} = 63.502\ \Omega$ at $f = 20.402$ GHz, and then grows dramatically to $Z_{odd} = 250.23\ \Omega$ at the asymptotic frequency $f_{so} = 59.329$ GHz. It is worthwhile to note that the odd-mode characteristic impedance has a variation of only 8.8% below 20 GHz. For the case $d = 1.0$ mm, the odd-mode impedance is $Z_{odd} = 58.384\ \Omega$ at $f = 0.01642$ GHz, and increases to $Z_{odd} = 99.133\ \Omega$ at the asymptotic frequency $f_{so} = 48.958$ GHz. For the case $d = 2.0$ mm, the odd-mode impedance is $Z_{odd} = 58.857\ \Omega$ at $f = 0.00854$ GHz and increases to $Z_{odd} = 72.129\ \Omega$ at the asymptotic frequency $f_{so} = 33.184$ GHz. Apparently, at low frequencies, the characteristic impedances are almost the same for USPDMLs with different lattice constants. Nevertheless, it is more dependent on the corrugation depth b. Similarly, Fig. 5(b) shows the even-mode characteristic impedances. For the CDML, the characteristic impedance increases slowly from minimum numerical value $Z_{even} = 51.22\ \Omega$ at $f = 0.03593$ GHz to $Z_{even} = 57.175\ \Omega$ at $f = 81.4$ GHz, with a variation of about 10.4% within the whole band. Moreover, for the CDML, the characteristic impedance for even-mode is smaller than that for odd-mode at low frequencies and is larger at high

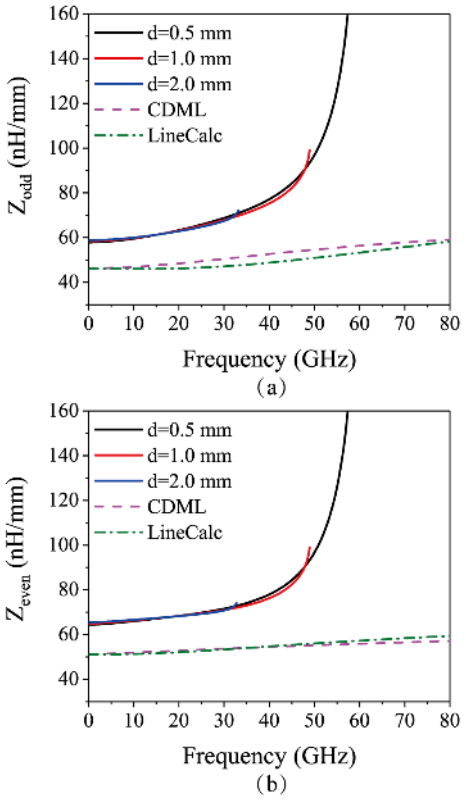


**FIGURE 5.** Characteristic impedances of USPDMLs for (a) odd-mode and (b) even-mode.

frequencies. The result from the *LineCalc* calculation agrees well with that obtained from the FEM one. For the USPDML with $d = 0.5$ mm, the even-mode impedance is $Z_{even} = 64.395\ \Omega$ at $f = 0.03015$ GHz, and increases to $Z_{even} = 250.23\ \Omega$ at the asymptotic frequency $f_{se} = 59.329$ GHz. For the cases $d = 1.0$ mm and $d = 2.0$ mm, the even-mode characteristic impedances have a minimal value of $Z_{even} = 64.876\ \Omega$ at $f = 0.01559$ GHz, and $Z_{even} = 65.469\ \Omega$ at $f = 0.00812$ GHz, respectively. According to [4], the relation between the odd-mode characteristic impedance $Z_{odd}$ and the differential signal characteristic impedance $Z_{diff}$ is given by

$$Z_{diff} = 2Z_{odd} \tag{5}$$

where the relation between even-mode characteristic impedance $Z_{even}$ and the common signal characteristic impedance $Z_{comm}$ is given by

$$Z_{comm} = Z_{even}/2 \tag{6}$$

We will verify the above numerical results using TDR measurement.

When the conductor ohmic loss of the transmission line is no longer negligible, the resistance per unit length should be calculated and the perturbation method is generally applicable [29]. The dissipation per unit cell on the metal surface of the differential microstrip lines can be calculated using tangential magnetic field $H_t$

$$P_d = \frac{1}{2}R_s \iint_s |H_t|^2 ds \tag{7}$$

where $R_s$ is the surface resistance, and the integral is made over the whole metal surface. The per unit cell resistance $R$ can be expressed as

$$P_d = \frac{1}{2}R|I|^2 \tag{8}$$

where $I$ is the surface current of the microstrip line.

Fig. 6 shows the per unit length resistance of the coupled microstrip lines. For the coupled conventional microstrip lines, resistance per unit length increases slowly with frequency and remains smaller than 0.1 Ω/mm over the frequency range investigated. In contrast, the resistance of the proposed USPDML rises sharply at $f \approx 30$ GHz, with larger resistance for smaller $d$. It can be seen that the resistance values for odd- and even-modes are approximately the same. The fact that the resistance rises sharply with frequency beyond 30 GHz indicates a much higher loss and longer rising time of the digital signals.

Moreover, if one further takes the substrate loss into account, the conductance $G$ becomes [30]:

$$G = \frac{\omega\varepsilon''}{|V_o|^2}R_s \iiint_v |E|^2 dv \tag{9}$$

with $\varepsilon''$ being the imaginary part of dielectric constant, $\omega$ being the angular frequency, $E$ is the electric field in the substrate (i.e., the integration is carried out over the substrate region), and $V_o$ being the voltage difference between the microstrip line and ground plane, respectively. Here, $\varepsilon''$ is further related to tan$\delta$ via:

$$\varepsilon = \varepsilon' - j\varepsilon'' = \varepsilon'(1 - jtan\delta) \tag{10}$$

Obviously, $G$ would increase with frequency. As a result, the dielectric loss can no longer be negligible at high frequencies. In our case, the loss tangent of RO4003 is equal to 0.0027. For the case of $d = 1.0$ mm, the values of $G_{odd}$ are about 0.0014916 S/m and 0.0149867 S/m for $f = 1$ GHz and $f = 10$ GHz, respectively. For $G_{even}$ the values are about 0.0014844 S/m and 0.0149385 S/m at $f = 1$ GHz and $f = 10$ GHz, respectively, confirming that $G$ increases with frequency and $G_{odd} \approx G_{even}$ in the present case.

For differential microstrip lines, it is necessary to consider the differential signal $S$-parameter $S_{dd}$ and common signal $S$-parameter $S_{cc}$. As the lattice constant of the periodic microstrip line is much smaller than the signal wavelength, the equivalent circuit used to describe infinitely small section in a uniform transmission line is still valuable [30], [31]. The circuit model of two coupled transmission lines can be used to simulate the $S$-parameters. Apparently, these equivalent circuit parameters will be frequency dependent and are denoted as $R(f)$, $L(f)$, $G(f)$ and $C(f)$. In order to check whether the circuit parameters obtained from the FEM simulations are indeed valid, the equivalent circuit of differential

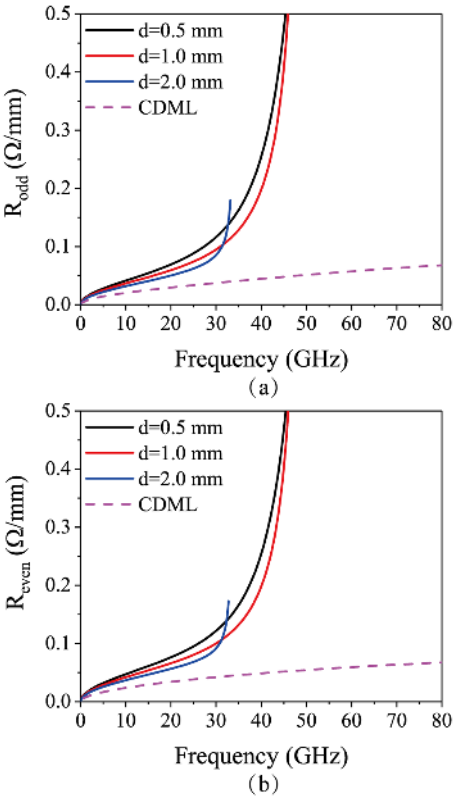


**FIGURE 6.** Resistance per unit length of USPDMLs for (a) odd-mode and (b) even-mode.

pair is used to calculate the *S*-parameters and compare the results with those obtained from the full-wave simulation. The total length and the lattice constant of the USPDML considered here is 10 cm and $d = 1.0$ mm, respectively. Fig. 7(a) and 7(b) show the signal transmission coefficient ($S_{dd21}$) and reflection coefficient ($S_{dd11}$) of the differential signal of the USPDML obtained from full-wave simulation (black line) and equivalent circuit model (red dashed and blue dotted line), respectively. Similarly, Fig. 7(c) and 7(d) are the transmission ($S_{cc21}$) and reflection ($S_{cc11}$) coefficients for the common signal. As is evident from Fig. 7, all the *S*-parameters obtained from the two methods are in excellent agreement. Since we use the model of conventional coupled transmission lines to fit the *S* parameters, the transmission line needs to be divided into many small segments during the fitting process. For comparison, two calculation schemes are employed here. In the first scheme, the subwavelength periodic coupled microstrip line is divided by the period length, and the calculated result is represented by red dashed line. In the second scheme, the division length is half period, and the obtained results are represented by blue dotted line. For the first division scheme, the deviation of $S_{dd21}$ between full-wave simulation and circuit model is 0.14 dB at 9.3 GHz. The *S*-parameters obtained from the second scheme fit well in the whole frequency range considered, the deviation between full-wave simulation and circuit model is merely 0.036 dB at 9.3 GHz. As expected theoretically, the smaller is the division length, the better does it fit with the result from the full-wave simulation. The conductance *G* is properly taken in the second scheme by referring to the equation (9.26) in Chapter 4 in the literature [4]. This remarkable consistency indicates that the obtained circuit parameters, namely *R*(*f*), *L*(*f*), *G*(*f*) and *C*(*f*), are reflecting the signals transmitting within the coupled microstrip lines in a precise manner. In addition, it is worthwhile to mention here, that the USPDML also exhibits significantly suppressed conversion effect between the differential and common signals.

## III. EXPERIMENTAL RESULTS

Being established the viability of the equivalent circuit model in extracting the circuit parameters that can satisfactorily reflect the signals transmitting in the USPDML, we next use the time domain TDR to measure the characteristic impedance of the differential and common signals of the USPDML. The two microstrip lines were connected to two ports of the TDR, then two step pulse signals with a phase difference of 180° were sent into the two ports, as depicted schematically in Fig. 1. The amplitude of the step pulse was 200 mV with a rising time of 30 ps. To match the simulation, the total length of the USPDML was also set at 10 cm. Fig. 8 shows the measured impedance for differential and common signals as a function of time for the USPDML with $d = 1.0$ mm (Fig. 8(d) and 8(e)) and $d = 2.0$ mm (Fig. 8(f) and (g)). The results for the CDML are also plotted for comparison (Fig. 8(b) and 8(c)). Fig. 8(a) also shows the optical photograph of the actual experimental sample. As has been pointed out

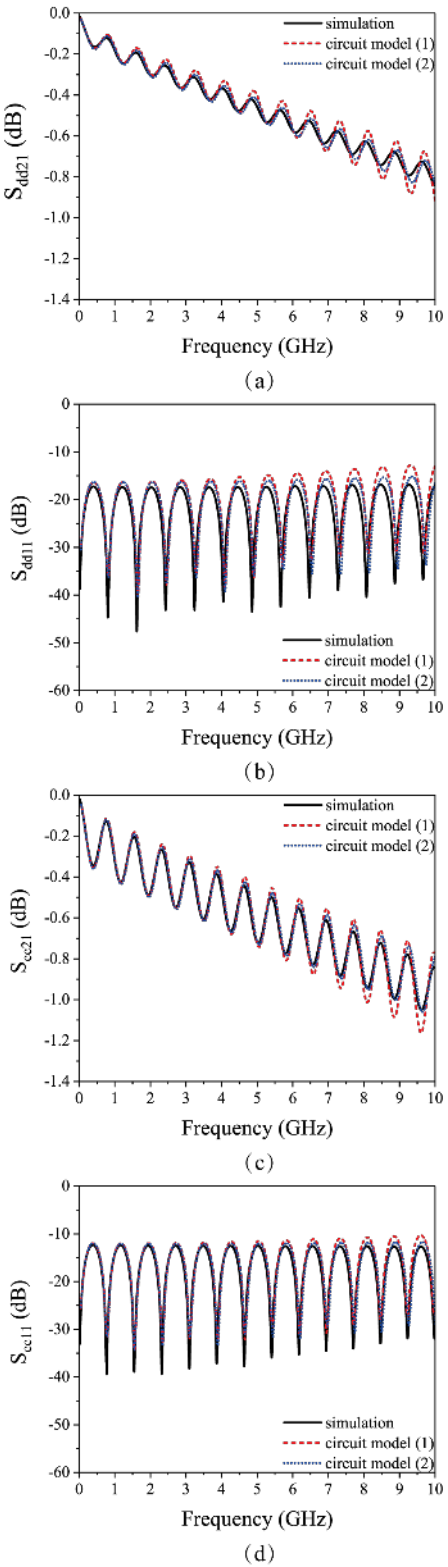


**FIGURE 7.** Frequency-dependent S-parameters of the USPDML. (a) Differential signal transmission coefficient $S_{dd21}$, (b) differential signal reflection coefficient $S_{dd11}$, (c) common signal transmission coefficient $S_{cc21}$, (d) common signal reflection coefficient $S_{cc11}$.

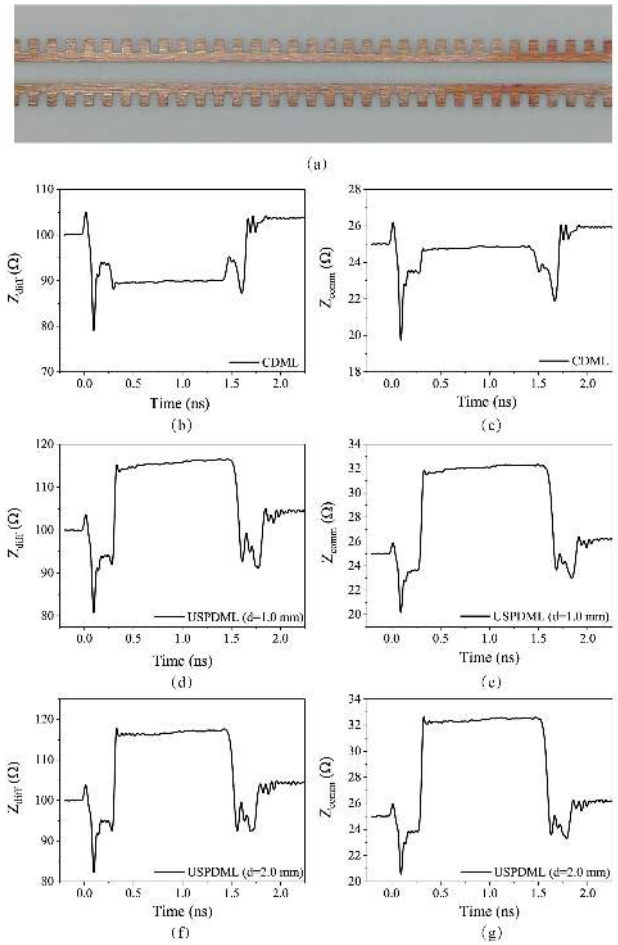


**FIGURE 8.** TDR measured results of USPDMLs. (a) Photo picture of the experimental USPDML sample. (b), (c) Differential signal and common signal impedances of the CDML; (d), (e) differential signal and common signal impedances of the USPDML with d=1.0 mm; (f), (g) differential signal and common signal impedances of the USPDML with d=2.0 mm.

by Oh et al. [32], when the loss is small, TDR can provide the information about the low-frequency characteristic impedance of the transmission line. Thus, when the time for the signal traveling over the transmission line is longer than its "rising time", the impedance measured by the TDR is primarily corresponding to the low-frequency characteristic impedance of the transmission line. As can be seen from Fig. 8(b), for the differential signal, the characteristic impedance of the CDML ranges from 89.52 to 90.13 Ω within the time spanning between 0.325 ns and 1.395 ns. Specifically, at $t$ = 1 ns, the measured characteristic impedance is 89.843 Ω, which is very close to the low-frequency numerical result of 92.472 Ω, giving a deviation of about 2.8%. Similarly, for the common signal (Fig. 8(c)), the measured characteristic impedance is between 24.63 and 24.9 Ω over the same time span and, at $t$ = 1 ns, the obtained value of 24.822 Ω has a difference of only 3% compared to the low-frequency numerical result of 25.61 Ω. In contrast, for the USPDML with $d$ = 1.0 mm, the characteristic impedance of the differential signal varies between 113.58 Ω and 116.23 Ω over the time span of 0.5–1.5 ns, as shown in Fig. 8(d). The value at $t$ = 1 ns is about 115.778 Ω, which has a difference of 0.786% as compared with the low-frequency numerical value of 116.696 Ω. Similarly, Fig. 8(e) indicates that the characteristic impedance of the common signal varies between 31.48 Ω and 32.34 Ω in the time interval of 0.5–1.5 ns and the value at $t$ = 1 ns is 32.098 Ω, which deviates about 1.05% from the numerical value of 32.438 Ω. Finally, for the USPDML with $d$ = 2.0 mm, the characteristic impedance of the differential signal varies between 116.56 Ω and 117.64 Ω over the similar time span, as shown in Fig. 8(f). The value at $t$ = 1 ns is 116.91 Ω, which deviates from the low frequency numerical value of 117.714 Ω by about 0.68%. The characteristic impedance of the common signal characteristic impedance varies between 32.07 Ω and 32.608 Ω, as shown in Fig. 8(g) and the value at $t$ = 1 ns is 32.489 Ω, which has an even smaller deviation of about 0.75% as compared with the numerical value of 32.7345 Ω. It is obvious from the results described above that the characteristic impedance of the USPDML performance such difference may be due to the etching error of the PCB substrate. It can be seen that the characteristic impedance of the USPDML is different from that of conventional differential microstrip lines and can be adjusted by the groove depth, line width, and lattice constant.

## IV. CONCLUSIONS

In summary, we have illustrated using the obtained circuit parameters, namely the equivalent per unit length capacitance, inductance, resistance and conductance, of USPDML from the equivalent circuit model, one can further derive both the differential signal and common signal characteristic impedances. Furthermore, the *S*-parameters calculated by using the equivalent circuit model and using the full-wave simulation exhibited excellent agreement with each other over a wide frequency range. For instance, during the frequency range (0–10 GHz), the results obtained from both methods showed a maximum deviation of merely 0.036 dB. The present results indicate that, in the low-frequency range (0–10 GHz), the proposed model is able to provide corresponding circuit parameters with adequate accuracy, which, in turn, enabled the implementation of structured differential microstrip lines in practical circuits. Indeed, even with possible defects originated from etching processes in fabricating a 10-cm-long USPDML on commercial printed circuit board, the characteristic impedance measured by TDR exhibited a maximum deviation from the numerical results by only about 1.05%. The proposed circuit model and the results presented in this paper, thus, pave an avenue for the engineers who are apt at implementing meta-materials into practical circuit applications.

## REFERENCES

[1] F. Xiao, W. Liu, and Y. Kami, "Analysis of crosstalk between finite-length microstrip lines: FDTD approach and circuit-concept modeling," *IEEE Trans. Electromagn. Compat.*, vol. 43, no. 4, pp. 573–578, Nov. 2001.

[2] D. A. Hill, K. H. Cavcey, and R. T. Johnk, "Crosstalk between microstrip

transmission lines," *IEEE Trans. Electromagn. Compat.*, vol. 36, no. 4, pp. 314–321, Nov. 1994.

[3] Y.-S. Sohn, J.-C. Lee, H.-J. Park, and S.-I. Cho, "Empirical equations on electrical parameters of coupled microstrip lines for crosstalk estimation in printed circuit board," *IEEE Trans. Adv. Packag.*, vol. 24, no. 2, pp. 521–527, Nov. 2001.

[4] E. Bogatin, *Signal and Power Integrity: Simplified*, 2nded., Upper Saddle River, NJ, USA: Prentice-Hall, 2009, pp. 475–553.

[5] F. D. Mbairi, W. P. Siebert, and H. Hesselbom, "High-frequency transmission lines crosstalk reduction using spacing rules," *IEEE Trans. Compon. Packag. Technol.*, vol. 31, no. 3, pp. 601–610, Sep. 2008.

[6] S. He, A. Z. Elsherbeni, and C. E. Smith, "Decoupling between two conductor microstrip transmission line," *IEEE Trans. Microw. Theory Technol.*, vol. 41, no. 1, pp. 53–61, Jan. 1993.

[7] L. Tani and N. El ouazzani, "Minimizing crosstalk on printed circuit board using non uniform guard traces," in *Proc. Int. Conf. Inf. Technol. Organizations Develop. (IT4OD)*,Fez, Morocc, 2016, pp. 1–4.

[8] B. R. Huang, K. C. Chen, and C. L. Wang, "Far-end crosstalk noise reduction using decoupling capacitor," *IEEE Trans. Electromagn. Compat.*, vol. 58, no. 3, pp. 836–848, Jun. 2016.

[9] S. Li, Y. Liu, Z. Song, and H. Hu, "Analysis of crosstalk of coupled transmission lines by inserting additional traces grounded with vias on printed circuit boards," in *Proc. Asia–Pacific Conf. Environ. Electromagn. (CEEM)*, Hangzhou, China, 2003, pp. 451–454.

[10] L. Zhi, W. Qiang, and S. Changsheng, "Application of guard traces with vias in the RF PCB layout," in *Proc. 3rd Int. Symp. Electromagn. Compat.*, Beijing, China, 2002, pp. 771–774.

[11] D. N. Ladd, and G. L. Gostache, "SPICE simulation used to characterized the cross-talk reduction effect to additional tracks grounded with vias on printed circuited boards," *IEEE Trans. Circuits Syst II: Analog Digit. Signal*, vol. 39, no. 2, pp. 342–347, Jun. 1992.

[12] I. Novak, B. Eged, and L. Hatvani, "Measurement and simulation of crosstalk reduction by discrete discontinuities along coupled PCB traces," *IEEE Trans. Instrum. Meas.*, vol. 43, no. 2, pp. 170–175, Apr. 1994.

[13] W. T. Huang, C. H. Lu, and D. B. Lin, "Suppression of crosstalk using serpentine guard trace vias," *Progr. Electromagn. Res.*, vol. 109, pp. 37–61, 2010.

[14] A. Suntives, A. Khajooeizadeh, and R. Abhari, "Using via fences for crosstalk reduction in PCB circuits," in *Proc. IEEE Int. Symp. Electromagn. Compat. (EMC)*, Portland, OR, USA, Aug. 2006, pp. 34–37.

[15] G. H. Shiue, G. Y. Chao, and R. B. Wu, "Guard trace design for improvement on transient waveforms and eye diagrams of serpentine delay lines," *IEEE Trans. Adv. Packag.*, vol. 33, no. 4, pp. 1051–1060, Nov. 2010.

[16] F. D. Mbairi,. W. P. Siebert, and H. Hesselbom, "On the problem of using guard traces for high frequency differential lines crosstalk reduction," *IEEE Trans. Compon. Packag. Technol.*, vol. 30, no. 1, pp. 67–74, March. 2007.

[17] S.-K. Lee, K. Lee, H.-J. Park, and J.-Y. Sim, "FEXT-eliminated tubal-ternated microstrip line for multi-gigabit/second parallel links," *Electron. Lett.*, vol. 44, no. 4, pp. 272–273, Feb. 2008.

[18] W. Jiang, X. D. Cai, B. Sne, and G. Wang, "Equation-based solutions to coupled, asymmetrical, lossy, and nonuniform microstrip lines for tab-routing application," *IEEE Trans. Electromagn. Compat.*, vol. 61, no. 2, pp. 548–557, Jan. 2019.

[19] W. Y. Yin, K. Kang, and J. F. Mao, "Electromagnetic-thermal characterization of on on-chip coupled (a)symmetrical interconnects," *IEEE Trans. Adv. Packag.*, vol. 30, no. 4, pp. 1051–1060, Nov. 2007.

[20] B. Pu, K. H. Kim, S. Y. Kim, and W. Nah, "Modeling and parameter extraction of coplanar symmetrical meander lines," *IEEE Trans. Electromagn. Compat.*, vol. 57, no. 3, pp. 375–383, Jun. 2015.

[21] A. R. Mallahzadeh, A. Ghasemi, S. Akhlaghi, B. Rahmati, and R. Bayderkhani, "Crosstalk reduction using step shaped transmission line," *Prog. Electromagn. Res. C*, vol. 12, pp. 139–148, 2010.

[22] J. J. Wu, "Subwavelength microwave guiding by periodically corrugated strip line," *Prog. Electromagn. Res.*, vol. 104, pp. 113–123, 2010.

[23] J. J. Wu et al., "Reduction of wide-band crosstalk for guiding microwave in corrugated metal strip lines with subwavelength periodic hairpin slits," *IET Microw. Antennas Propag.*, vol. 6, no. 2, pp. 231–237, Feb. 2012.

[24] X. Dai, W. Feng, and W. Che, "Reduction of UWB far-end crosstalk in microwave and millimeter-wave band of parallel periodically loaded transmission lines with discontinuous structured guard lines," *IEEE Trans. Plasma Sci*, vol. 48, no. 7, pp. 2372–2383, July, 2020.

[25] F. Grassi, P. Manfredi, X. K. Liu, J. K. Sun, X. L. Wu, D. V. Ginste, and S. A. Pignari, "Effects of undesired asymmetries and nonuniformities in differential lines," *IEEE Trans. Electromagn. Compat.*, vol. 59, no. 5, pp. 1613–1624, Nov. 2017.

[26] G. H. Shiue, J. H. Shiu, Y. C. Tsai, and C. M. Hsu, " Analysis of common-mode noise for weakly coupled differential serpentine delay microstrip line in high-speed digital circuits," *IEEE Trans. Electromagn. Compat.*, vol. 54, no. 3, pp. 655–666, Jun. 2012.

[27] J. J. Wu, D. J. Hou, K. Liu, L. Shen, C. A. Tsai, C. J. Wu, D. C. Tsai, and T. J. Yang, "Differential microstrip lines with reduced crosstalk and common mode effect based on spoof surface plasmon polaritons," *Opt. Express*,22(22), 26777–26787, 2014.

[28] H. Takeda, K. Iokibe, and Y. Toyota, "Crosstalk suppression by introducing periodic structure into differential transmission lines," IEICE Trans. on comm. J-101-B, 212-219, 2018.

[29] R. E. Collin, *Foundation for microwave engineering*, 2nded., New York:McGraw-Hill ,1992, pp. 550–551.

[30] D. M. Pozar, *Microwave Engineering*, 3rded., Hoboken, NJ, USA: John Wiley Sons, 2005, pp. 51–52.

[31] C. R. Paul, *Analysis of multi-conductor transmission lines*, 2nded., Hoboken, NJ, USA: John Wiley Sons, 2005, pp. 18–19.

[32] K. S. Oh et al., *High-speed signaling jitter modeling, analysis, and budgeting*,Upper Saddle River, NJ, USA: Prentice-Hall, 2012, pp. 121–136.

CHIA HO WU was born in Tainan, Taiwan. He received the M. S. degree in physics from National Tsing Hua University, Hsinchu, Taiwan, in 1987, and the Ph.D. degree in electro-optics from Chiao Tung University, Hsinchu, Taiwan, in 1997. He is a Professor of Department of Applied Physics, College of Science, Zhejiang University of Technology, Hangzhou, China from 2018. His research interests include propagation and scattering of dielectric waveguides, numerical analysis of dielectric gratings, active leaky wave antennas and subwavelength periodic metal structures.

GUOBING ZHOU was born in Huzhou,Zhejiang, China, in 1994. He received the B.S. degree from the Zhejiang University of Technology, Zhejiang, China, in 2017.Now he is working towards a master's degree in this university. His interests include microwave, millimeter-wave and subwavelength periodic structures.

JENH-YIH JUANG was born in Tainan, Taiwan in 1957. He received the B. S. and M. S. degrees in materials science from National Tsing Hua University, Hsinchu, Taiwan, in 1979 and 1981, respectively. He received the Ph.D. degree in electronic materials from Massachusetts Institute of Technology in 1989. He joined the Department of Electrophysics, National Chiao Tung University, Hsichu, Taiwan in 1989 as an associate professor. He became a full professor since 1993. His research interests are mainly on experimental condensed matter physics, including superconductivity, colossal magnetoresistance and multiferroic manganites, topological insulators etc.

QIAN SHEN was born in Sichuan Province, China, on September 13, 1994. She received the B.S., M.S., and Ph.D. degrees from Nanchang University, Nanchang, China, in 2014, 2017, and 2020, respectively. Her research interests are in surface magnetoplasmon, unidirectional wave transmission, and terahertz time domain spectroscopy.

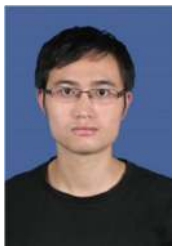

YUN YOU was born in Jiangxi Province, China, 1990. He received the B.S., M.S., and Ph.D. degrees from Nanchang University, Nanchang, China, in 2012, 2015, and 2019, respectively. He works at Department of Applied Physics, College of Science, Zhejiang University of Technology, Hangzhou, China since 2020. His research interests are in surface magnetoplasmons, one-way waveguide, and 2D materials.

JINHUA YAN was born in Nantong, China. He received the B.S. degree in Physics in 2002 and the Ph.D. degree in Optical Engineering in 2007 from Zhejiang University, Hangzhou, China, respectively. He is an associate professor of the Department of Applied Physics, College of Science, Zhejiang University of Technology, Hangzhou, China. His research interests include nano-photonic devices, numerical analysis of surface structure-based photonic devices, and optical sensing technique and application.

LINFANG SHEN was born in Zhejiang, China, in 1965. He received the B.S. degree in physics from Peking University, Beijing, China, in 1986, the M.S. degree in plasma physics from the Institute of Plasma Physics, Academy of Science of China, Hefei, China, in 1989, and the Ph.D. degree in electronic engineering from University of Science and Technology of China in 2000. He is currently a professor with Zhejiang University of Technology. His present research interests are in surface plasmonics, photonic crystals, and metamaterials.

HANG ZHANG was born in Zhejiang, China. He received the Ph.D. degree in physics from Zhejiang University, Hangzhou, China, in 2002. He is an associate professor of Department of Applied Physics, College of Science, Zhejiang University of Technology, Hangzhou, China. His research interests include freeform optical design, semiconductor illumination and the propagation of subwavelength periodic metal structures.

YU WU received the B.S. degree in physics from Fuyang Normal University, Fuyang , Chin, in 2019. She is currently pursuing the M.S. degree from College of Science, Zhejiang University of Technology, Hangzhou, China. Her current research interests include microwave theory, surface plasmon, and antennas.

FANGMING ZHU was born in Zhejiang, China, in 1969. She received the B.S. degree in communication engineering from Electronic Science and Technology University, Xi'an, China, in 1991, the M.S. degree in radio engineering from SouthEast University, Nanjing, China in 1994, and the Ph.D. degree in optic engineering from Zhejiang University of China in 2004. She is currently an associate professor with Hangzhou Normal University. Her research interests include surface plasmonics, metamaterials, and antennas.

CHIN-CHIH CHANG received the M.S. degree in engineering science from National Cheng Kung University, Tainan, Taiwan, in 1990 and the Ph.D. degree in computer science from Oklahoma State University, USA, in 2000. He is an assistant professor in the Department of Computer Sciences and Information Engineering, Chung Hua University, Hsinchu City, Taiwan. His research interests include deep learning, recommendation systems, context-aware computing, sensor and Internet of Things (IoT) implementation.